Impact of Air Void Content on the Viscoelastic Behavior of Hot Mix Asphalt

B. Hofko, R. Blab & M. Mader
Vienna University of Technology, Institute of Transportation, Research Center of Road Engineering, Vienna, Austria

ABSTRACT: Volumetric mix design properties of hot mix asphalt (HMA) have a significant impact on the viscoelastic behavior of the material. This study presents results from an extensive lab testing program on two different HMAs: an asphalt concrete (AC) with a maximum aggregate size of 22 mm and an unmodified bitumen 50/70, as well as an AC 22 with an SBS-modified binder PmB 45/80-65. For both materials the dynamic modulus |E*| and the phase lag φ were obtained by testing specimens in the 4-point-bending beam test (4PBB) and the direct tension and compression test (DTC). The stiffness tests were run with a temperature and frequency sweep. Since the air void content of the specimens was varied in a wide range, the impact of this volumetric mix design property on the viscoelastic behavior can be analyzed in detail. It was found that the time-temperature superposition principle (TTSP) can be extended to an air void-time-temperature superposition (AVTTSP) where the viscoelastic behavior of HMA can be derived for an arbitrary air void content at a chosen reference temperature and reference frequency. In addition results from the two test setups (4PBB and DTC) used within the study are compared and discussed.

1 INTRODUCTION

Air voids have a significant influence on the performance of HMA. Several research projects in the past studied the effect of air voids on different performance parameters (Bell et al. 1984; Linden et al. 1988; Harvey et al. 1994 and Harrigan 2002). More recently (Youngguk et al. 2007) presented an air void model for performance prediction of HMA, and (You et al. 2010) studied the effects of air voids on 2D and 3D discrete element models. (Kassem et al. 2011) worked on the influence of air voids on the resistance to fatigue cracking, permanent deformation and moisture damage. From the results presented in these studies, it can be concluded that the dynamic modulus of HMA tends to decrease with increasing void content and the phase lag φ characterizing the viscosity of the material tends to increase with increasing void content. Thus, HMAs react less stiff and more viscous to loading when the content of air voids increases.

Since the behavior of viscoelastic materials is influenced by temperature as well as time (i.e. frequency of loading), its parameters like the dynamic modulus and phase lag are a function of time and temperature, e.g. $|E^*| = |E^*|(t,T)$. One way to describe this function is to carry out a number of dynamic tests at large number of temperatures and frequencies. For so-called thermo-rheological simple materials like HMA, there is a more efficient way. For these materials, time and temperature can be combined to one parameter. When dynamic tests are carried out on a thermo-rheological simple material at different temperatures, the results show the same function in terms of time if the time domain is scaled. A lower temperature leads to a shift of mate-

rial parameters to shorter times or higher frequencies. A master curve can be derived from a limited number of tests at different temperatures and frequencies by taking advantage of the time-temperature superposition principle (TTSP). This means that the viscoelastic parameters can be obtained for an arbitrary temperature and a wide range of frequencies, without having to test the material at this specific temperature or frequency (Findley et al., 1989). (Rowe et al. 2009) showed that the shape of master curves is significantly affected by the air void content of an HMA.

2 OBJECTIVES AND TASKS

The main objective of the presented study was to combine the effect of time, temperature and air void content on the viscoelastic behavior of HMA under dynamic loading. The TTSP includes the effect of time and temperature. From previous studies mentioned above it seemed that there should be a further link to also include the air void content into the TTSP and extend it to an air void-time-temperature superposition principle (AVTTSP). To achieve this objective, the following tasks were carried out:

- Produce HMA-slabs by roller compaction in the lab with different target contents of air voids and obtain specimens from the slabs by coring and cutting for stiffness tests.
- Conduct stiffness tests on the specimens with different contents of air voids with temperature and frequency sweep.
- Analyze results in terms of dynamic modulus |E*| and phase lag φ at different temperatures, frequencies and air void contents.
- Develop master curves combining the effect of time, temperature and air void content by introducing the AVTTSP.
- Discuss results gathered from different HMAs and different test setups.

3 MATERIALS AND SPECIMEN PREPARATION

Two different HMAs were tested in the project: An asphalt concrete (AC) with a maximum aggregate size of 22 mm with unmodified bitumen 50/70 (penetration between 50 $^{1}/_{10}$ mm and 70 $^{1}/_{10}$ mm), referred to as AC 22 50/70 and an AC 22 with an SBS-modified bitumen PmB 45/80-65 (penetration between 45 $^{1}/_{10}$ mm and 80 $^{1}/_{10}$ mm, softening point > 65°C). The mineral type used for both mixes is crushed limestone.

Sieve Size [mm]	Percentage Passing [% (m/m)]		
	MV	min	max
0.0625	6.9	8.2	6.4
0.125	8.4	9.8	7.8
0.25	10.6	12.0	10.0
0.5	13.7	15.8	13.4
1	19.6	22.9	19.0
2	30.3	32.8	29.3
4	42.1	45.2	40.6
8	59.1	61.9	56.1
11.2	70.6	74.0	69.2
16	83.0	85.4	82.4
22.4	97.4	98.5	96.6
31.5	99.8	99.8	99.7

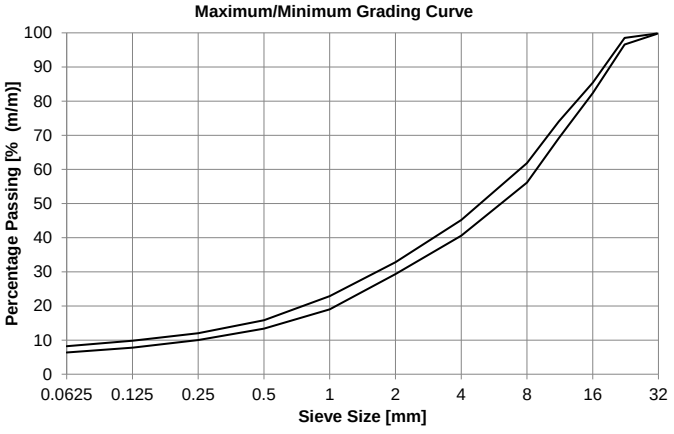

Figure 1: Mean value, minimum and maximum of the gradation (left table) and graphical representation of minimum and maximum grading curve (right figure).

For the test program a total of 69 slabs were compacted from the two mixes. The mean value (MV) of the grading curves of all 69 slabs is given in the table in Figure 1. The table contains the minimum and maximum grading curve as well. The right diagram in Figure 1 shows the maximum and minimum grading curve. The given data show that the difference in gradation be-

tween the slabs is small with a maximum difference between minimal and maximal grading curve of 3.5% (m/m). Thus, it can be assumed that the grading curve does not influence the results presented in the further course.

The binder content for both mixes was set to 4.5% (m/m), which is the optimal binder content according to Marshall.

HMA slabs were produced in the lab by roller compaction in a path-controlled way to a specified target density. The dimensions of the slabs are 500x260 mm with a variable height. For specimens tested in both setups (4PBB and DTC) the height of the slabs was set to 80 mm. For 4PBB, 3 prismatic specimens (500x60x60 mm) were cut from each slab according to the pattern shown in the left picture in Figure 2. The x-direction of the co-ordinate system shows the path of the roller compactor, the z-axis marks the direction of the compaction force. For DTC, 6 cylindrical specimens (Ø = 63.5 mm, H = 200 mm) were cored and cut from each slab. The pattern is depicted in the right picture in Figure 2.

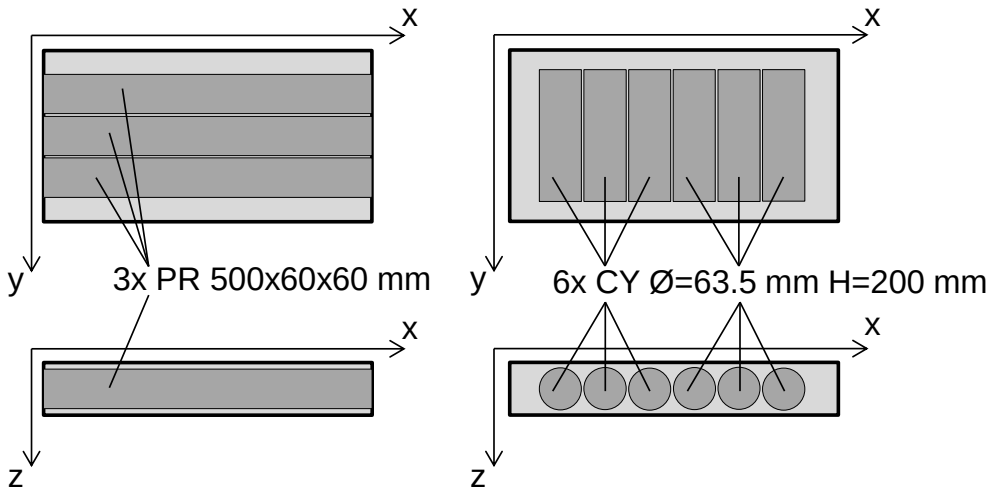

Figure 2: 4PBB specimens cut from HMA-slabs (left) and DTC-specimens cored and cut from HMA-slabs (right).

Table 1 shows the number of slabs produced for each HMA and each test setup. It also contains information on how many specimens were tested.

Table 1: Number of slabs produced for testing and number of tested specimens.

	Number of slabs produced (number of tested specimens)	
	4PBB	DTC
AC 22 50/70	34 (88)	10 (52)
AC 22 PmB 45/80-65	23 (67)	9 (51)

The bulk density and the volume of air voids were determined for each specimen. The left diagram in Figure 3 shows the distribution of the air void content for specimens tested in the 4PBB for both mixes. Each bar represents a percentage of specimens which lies within a range of air voids. Obviously, specimens from the AC 22 50/70 exhibit a wide range in terms of air void content ranging from 1.0% (v/v) up to 7.0% (v/v). The distribution for specimens from AC 22 PmB 45/80-65 shows less scattering. Still, specimens with an air void content ranging from 2.0% (v/v) to 5.0% (v/v) can be found. The right diagram in Figure 3 presents analogous data for specimens tested in the DTC. The air void distribution is narrower than for the specimen tested in 4PBB. Specimens from AC 22 50/70 range from 2.0% (v/v) to 5.0% (v/v) and specimens from AC 22 PmB 45/80-65 range from 1.5% (v/v) to 4.0% (v/v).

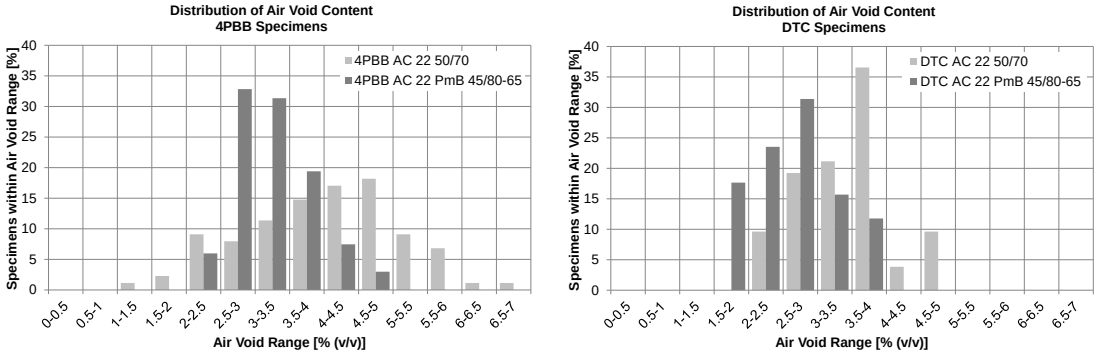

Figure 3: Distribution of air void content for specimens tested in 4PBB (left) and DTC (right).

4 TEST METHODS AND TEST CONDITIONS

To investigate the viscoelastic behavior of HMA two different test setups were employed. In the 4PBB, the specimen is subjected to dynamic (sinusoidal) flexural loading perpendicular to its longitudinal axis. Figure 4 shows the principle of the setup. While the two outer supports of the specimen are fixed and allow rotation and translation in horizontal direction, the bending is realized by the two inner supports in vertical direction perpendicular to the longitudinal axis of the specimen. The test device is located within a temperature chamber to control the test temperature throughout the test. The sinusoidal bending is carried out deformation-controlled symmetrically around the zero position with a constant amplitude. In order not to damage the specimen during stiffness testing, the amplitude of the horizontal strain on the lower side of the specimen is set to 50 µm/m. The deformation of the specimen in vertical direction as well as the loading is recorded as a function of time.

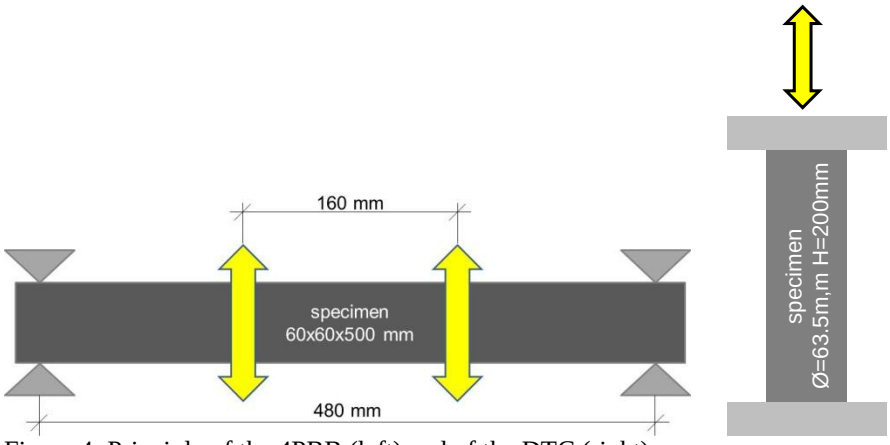

Figure 4: Principle of the 4PBB (left) and of the DTC (right).

The DTC represents another test setup to assess the viscoelastic behavior of HMA. The principle is shown in Figure 4. The specimen is fixed to two load plates on both of its end planes. The specimen is subjected to cyclic (sinusoidal) axial loading around the zero position. The test is carried out deformation controlled with a strain amplitude of 10 µm/m in order not to damage the specimen during the stiffness test. Again, the device is located within a temperature chamber to control the test temperature.

For both test setups, the dynamic modulus |E*|, as well as the elastic (E_1) and viscous (E_2) part of the dynamic modulus and the phase lag (φ) can be obtained according to the following equation (Di Benedetto et al. 2001) and the definition shown in Figure 5.

$$
\begin{aligned}
E^* &= \frac{\sigma_0}{\varepsilon_0} \cdot \left(\cos\varphi + i \cdot \sin\varphi\right) = E_1 + i \cdot E_2 \\
E_1 &= \frac{\sigma_0}{\varepsilon_0} \cdot \left(\cos\varphi\right) \\
E_2 &= \frac{\sigma_0}{\varepsilon_0} \cdot \left(\sin\varphi\right) \\
\left|E^*\right| &= \sqrt{E_1^2 + E_2^2} = \frac{\sigma_0}{\varepsilon_0}
\end{aligned}
\tag{1}
$$

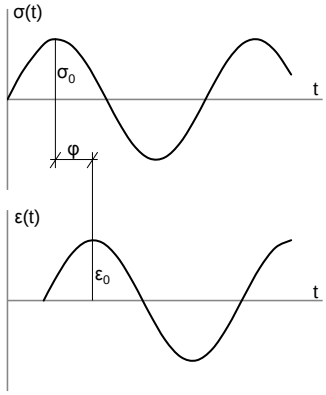

Figure 5: Stress and strain for a viscoelastic material as a result of cyclic tests.

Tests with both setups were run at temperatures of -10°C, +5°C and +20°C and frequencies ranging from 0.1 Hz to 40 Hz. At the end of each test a second frequency packet of 0.1 Hz was run and test results in terms of dynamic modulus were compared to the results of the first 0.1 Hz frequency package. If the results of the last and first 0.1 Hz packet exhibited a difference larger than 5%, the test results were not considered for further analysis since it is assumed that the specimen was subject to fatigue in the course of testing.

5 AIR VOID-TIME-TEMPERATURE SUPERPOSITION

The TTSP takes advantage of the fact that time (i.e. testing frequency) and temperature are interchangeable variables for thermo-rheological simple materials like HMA. This means that an increase in temperature is equal to a decrease in frequency in terms of viscoelastic material behavior, vice versa. The TTSP is a powerful concept to derive a single master curve from material tests carried out at different temperatures and frequencies for a user-defined reference temperature and a wide range of frequencies. Thus, the master curve enables the user to obtain viscoelastic material parameters even for not tested temperatures and frequencies (Findley et al. 1989).

The following section aims towards an extension of the TTSP to include another variable into the concept, in this case the air void content of the HMA. By using the air void-time-temperature superposition principle (AVTTSP), viscoelastic material parameters can be derived for a reference temperature and reference frequency for a wide range of air void contents. The derivation of the AVTTSP is presented exemplarily for the AC 22 50/70 tested in the 4PBB in the following.

When the impact of time and air void content on the dynamic modulus are taken into consideration at a constant temperature of 20°C (see left diagram in Figure 6) it is obvious that an increase in frequency leads to an increase in the dynamic modulus. If the focus is laid upon the air void content, the dynamic modulus decreases with increasing void content. The decrease of the dynamic modulus can be approximated by a linear for each test frequency, although the linearity tends to decrease with decreasing frequency. At 40 Hz the linear regression of the modulus vs. air void content exhibits a coefficient of determination R^2 of 0.8528. R^2 drops to 0.59 for

a frequency of 0.1 Hz. The sensitivity of the material stiffness in terms of dynamic modulus to a change in the air void content increases with increasing frequency. At 0.1 Hz the slope of the linear is -273.87 and increases by a factor of 2.6 to -709.45 at 1.0 Hz and by a factor of 1.75 to -1241 at 10 Hz. The slope of the linear reaches a maximum at 40 Hz with -1400.2. The more time the material is given to react to loading, the less important becomes the air void content. Since the elastic part of the material behavior is more dominant at high frequencies, it can be stated that the elastic material behavior is more sensitive to a change in the air void content.

Analogous to the TTSP, it is possible to scale the air void content of test results at different frequencies to derive one single master curve for a reference frequency for one test temperature. The equation for this shifting procedure, which can be called air void-time superposition, is

$$VC_f = VC + a_f \cdot (\ln f_0 - \ln f) \mid VC_f \geq 0 \tag{2}$$

where VC_f = scaled void content in the air void-time superposition [% (v/v)]; VC = void content [% (v/v)]; a_f = shift factor depending on test frequency; f_0 = reference frequency [Hz]; f = test frequency [Hz].

The procedure explained above was carried out for test data shown in the left diagram in Figure 6. The right diagram in Figure 6 shows the master curve for a reference frequency of 10 Hz. The shift factor a_f was determined to be 1.3. The shape of the master curve resembles one part of an S-shaped sigmoidal function. This is analogous to the master curve according to the TTSP. At higher void contents the dynamic modulus converges towards zero asymptotically. By employing the air void-time superposition the material behavior can be determined for a wide range of air void contents at the test temperature for a reference frequency.

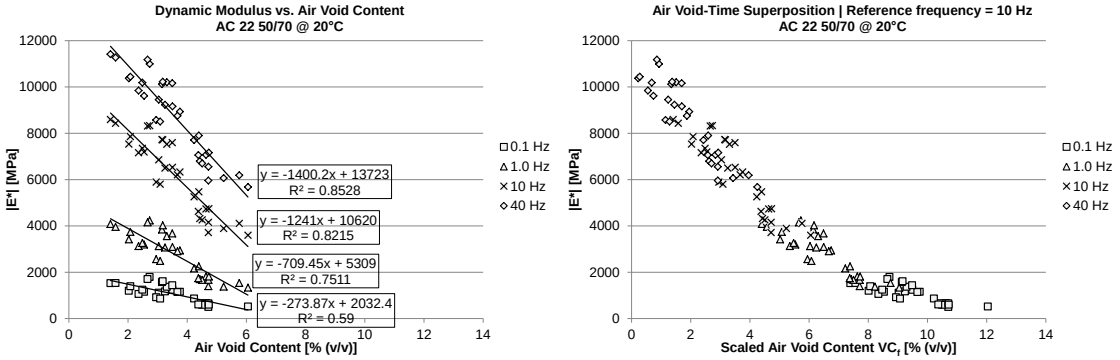

Figure 6: Dynamic modulus for different frequencies and air void contents at 20°C for the AC 22 50/70 tested in the 4PBB (left) and air void-time superposition (right).

When test data is available for more than one test temperature, the air void-time superposition can be extended even more. The left diagram in Figure 7 shows master curves according to the air void-time superposition for stiffness tests carried out on the AC 22 50/70 in the 4PBB at temperatures of -10°C, +5°C and +20°C. The reference frequency was set to 10 Hz. Again, these master curves can be shifted in the air void domain to create a more general master curve including test data for all test temperatures and frequencies. This air void-time-temperature superposition (AVTTSP) is presented in the right diagram in Figure 7 and can be derived according to the following equation:

$$VC_{f,T} = VC + a_f \cdot (\ln f_0 - \ln f) + a_T \cdot (\ln T_0 - \ln T) \mid VC_{f,T} \geq 0 \tag{3}$$

where $VC_{f,T}$ = scaled void content in the AVTTSP [% (v/v)]; a_T = shift factor depending on test temperature; T_0 = reference temperature [K]; T = test temperature [K].

By employing the AVTTSP, the viscoelastic material behavior can be determined for an even wider air void range at a reference temperature and a reference frequency. Two shift factors have to be determined. The best way to derive these two shift factors is to start with the shift factor a_f, which is dependent on the test frequency and continue with the shift factor a_T, which

depends on the test temperature. It was found that one set of shift factors describes the behavior of a material tested at different frequencies and temperatures. For the presented example of an AC 22 50/70 tested in the 4PBB, the shift factor a_f was found to be 1.3 and the shift factor a_T to be -140.

The right diagram in Figure 7 shows the master curve according to the AVTTSP for a reference frequency of 10 Hz and a reference temperature of -10°C. The master curve presented in the right diagram in Figure 7 states that an increase in the void content is equal to an increase in test temperature or a decrease in test frequency. The AVTTSP gives valuable information on how a material reacts to dynamic loading when the air void content of the material is changed. Thus, it can be used for a sensitivity analysis in terms how an increase in the void content affects the viscoelastic material behavior. It can also be used for quality assurance in the field when the void content of samples taken from a pavement is determined in accompanying quality control.

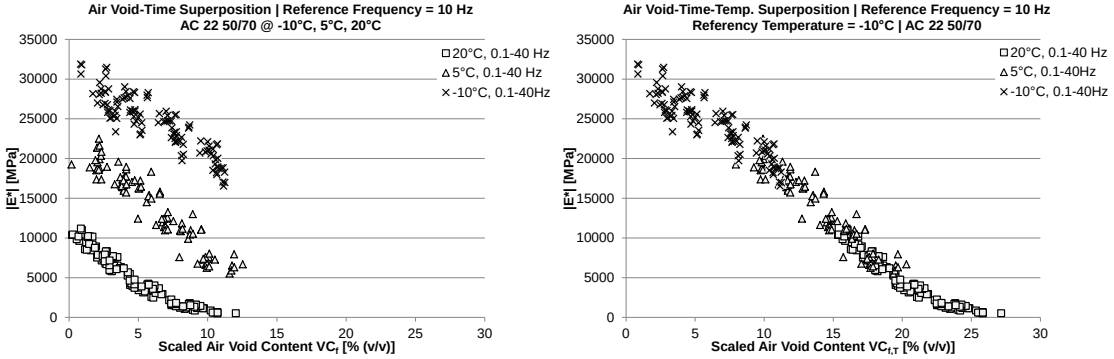

Figure 7: Air void-time superposition at different temperatures for AC 22 50/70 tested in the 4PBB (left) and air void-time-temperature superposition (AVTTSP) (right).

The left diagram in Figure 8 shows the same master curve as the right diagram in Figure 7 but the dynamic modulus is shown in log scale. The right diagram in Figure 8 contains the master curve of the phase lag φ according to the AVTTSP for the same test data as presented above. The shift factors are the same as for the dynamic modulus. The presented data prove that the AVTTSP is also valid for the phase lag φ. Again the master curve was determined for a reference frequency of 10 Hz and a reference temperature of -10°C. An increase in the void content goes along with an increase in the viscosity of the material. The master curve also shows that an increase in the void content at a specific reference frequency and temperature has the same effect as an increase of the test temperature or decrease in test frequency at a constant void content.

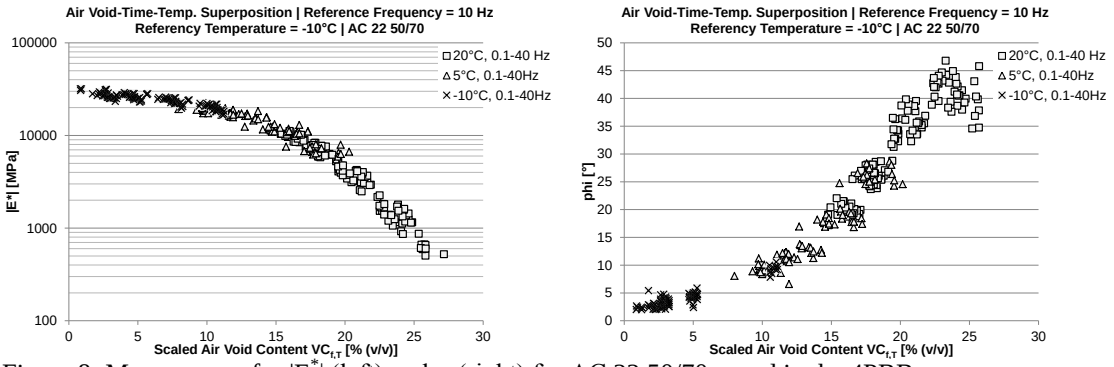

Figure 8: Master curve for $|E^*|$ (left) and φ (right) for AC 22 50/70 tested in the 4PBB.

6 RESULTS AND DISCUSSION

Since two different mixes were tested with two different test setups, an analysis of the difference between mixes and test setups is presented in the following. Table 2 and Table 3 show the shift factors a_f and a_T for both mixes and test setups. The master curves presented in the following are always for a reference frequency of 10 Hz and a reference temperature of -10°C.

Table 2: Shift factor a_f for the two mixes and test setups.

a_f	4PBB	DTC
AC 22 50/70	1.27	1.10
AC 22 PmB 45/80-65	1.40	1.10

Table 3: Shift factor a_T for the two mixes and test setups.

a_T	4PBB	DTC
AC 22 50/70	-140	-135
AC 22 PmB 45/80-65	-133	-140

Figure 9 shows the master curves of the dynamic modulus (right diagram) and the phase lag (left diagram) for the two mixes, AC 22 50/70 and AC 22 PmB 45/80-65, tested in the 4PBB. The material stiffness in terms of the dynamic modulus is comparable for both materials in the low and high air void range. Between air void contents of 5.0% (v/v) and 20.0% (v/v), the mix with the modified binder exhibits lower stiffness. When it comes to the phase lag, both materials behave similar in the low air void range. In the intermediate air void range from 5.0% (v/v) to around 20% (v/v) the mix with the unmodified binder shows lower phase lags and is thus more elastic than the mix with the PmB. This situation is turned around for air void contents above 20.0% (v/v). The PmB mix seems to reach a threshold value of around 30° to 35°, whereas the unmodified mix ranges between 35° and 45°. This goes along with the fact that mixes with PmB exhibit more elastic behavior in the high temperature or low frequency range which is equal to a high air void range.

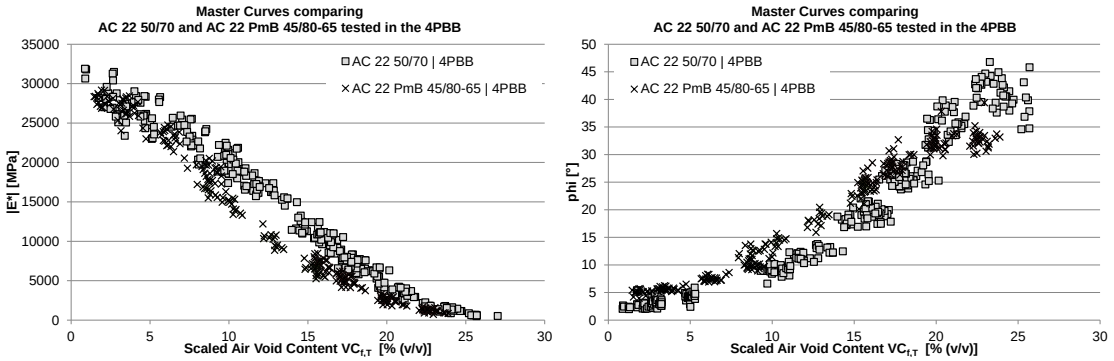

Figure 9: Master curves of |E*| (left) and φ (right) comparing AC 22 50/70 and AC 22 PmB 45/80-65 tested in the 4PBB.

When both mixes are tested in the DTC, no clear difference between the materials can be seen. Figure 10 shows the results. Both mixes exhibit similar dynamic moduli throughout the air void contents. In terms of the phase lag (right diagram in Figure 10), the situation is similar to the results from 4PBB testing. The unmodified mix shows lower phase lags in the low air void range up to 15.0% (v/v) and higher phase lags in the high air void range from around 20.0% (v/v) on.

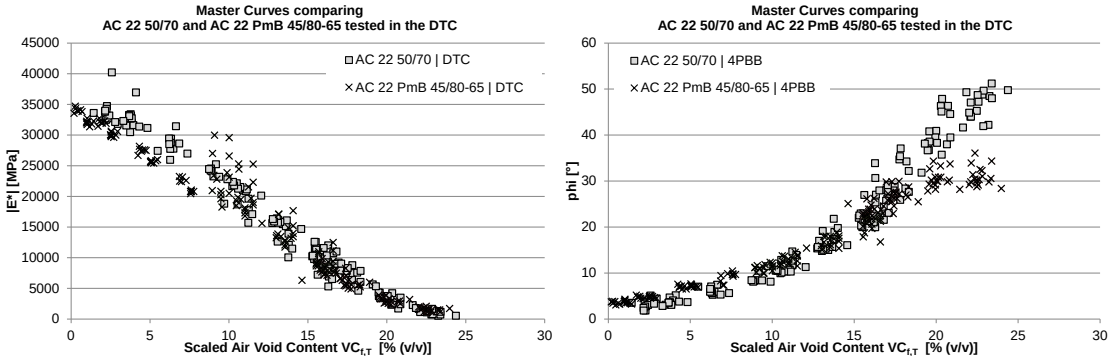

Figure 10: Master curves of |E*| (left) and φ (right) comparing AC 22 50/70 and AC 22 PmB 45/80-65 tested in the DTC.

The two diagrams in Figure 11 compare results for the AC 22 50/70 tested in the 4PBB and the DTC. The left diagram shows the master curves for the dynamic modulus. For the low air void range (equal to low temperatures or high frequencies) the material reacts stiffer when tested in axial direction in the DTC. From around 10.0% (v/v) on both test setups result in similar dynamic moduli. The opposite tendency can be seen in terms of the phase lag (right diagram in Figure 11). In the low air void range up to around 10.0% (v/v) both setups produce similar phase lags. When the air void content is increased further, specimens tested in the DTC react more viscous, i.e. produce higher phase lags than specimens tested in the 4PBB. Thus, it can be stated that both setups produce comparable results in terms of material stiffness in the high air void range and in terms of viscosity in the low air void range.

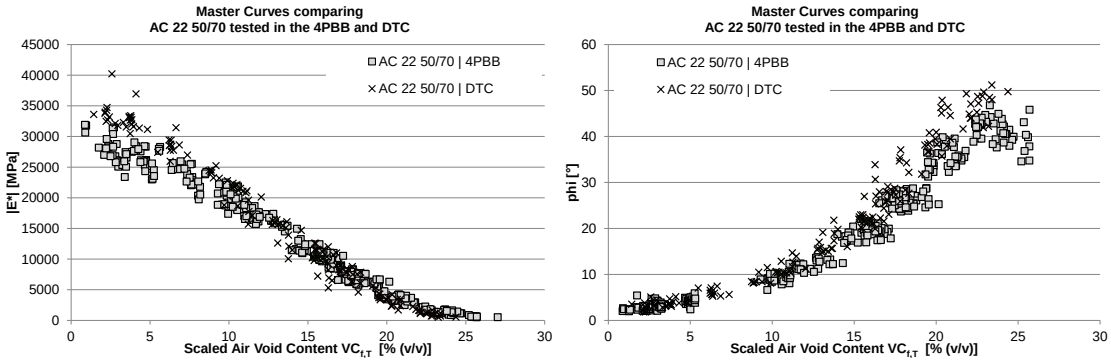

Figure 11: Master curves of |E*| (left) and φ (right) comparing AC 22 50/70 tested in the 4PBB and DTC.

Figure 12 shows an analogous comparison of test setups for the AC 22 PmB 45/80-65. The left diagram contains data for the dynamic modulus. Interestingly enough there is no difference between both setups if the intermediate range of the air void content is left out of the consideration for the DTC test data. Due to problems in the test control this data shows large scattering and cannot be seen as valid. When the focus is put upon the phase lag (right diagram in Figure 12) it seems that the modified mix tested in the DTC results in slightly lower phase lags in the intermediate air void range (from 10.0% (v/v) to 20.0% (v/v)).

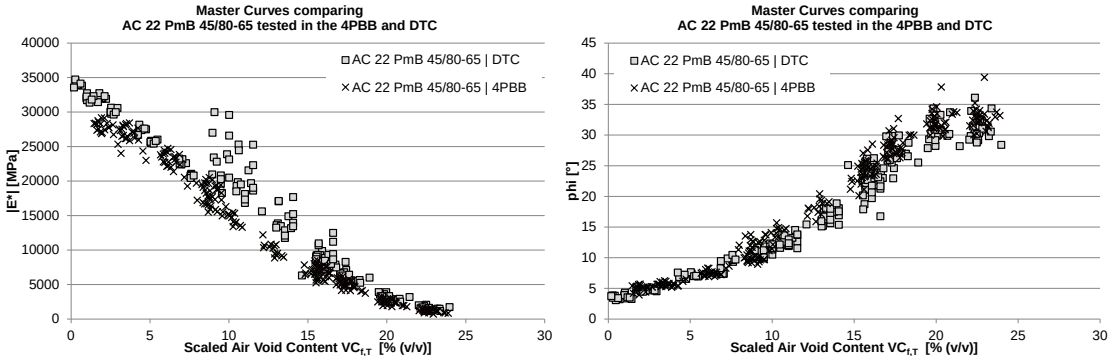

Figure 12: Master curves of |E*| (left) and φ (right) comparing AC 22 PmB 45/80-65 tested in the 4PBB and DTC.

7 SUMMARY AND CONCLUSIONS

The presented research study aimed towards an extension of the TTSP to include the effect of the air void content of HMA into the superposition principle. Therefore, two different HMAs, an AC 22 50/70 and an AC 22 PmB 45/80-65, were tested in dynamic stiffness tests with two different setups, the 4PBB and the DTC. The specimens were obtained by cutting and coring from HMA slabs compacted with a roller compactor. A total of 69 HMA slabs were produced with a wide range of air void contents to investigate the impact of this volumetric mix design property on the viscoelastic material behavior in terms of dynamic modulus and phase lag. The dynamic stiffness tests were carried out with temperature and frequency sweep.

From the test results it can be concluded that there is a linear interrelation between the dynamic modulus and the air void content for all test frequencies. A higher void content leads to lower material stiffness (i.e. dynamic modulus). The linearity is more significant for high frequencies than for low frequencies. In addition the HMA reacts more sensitive to a change in the void content the higher the test frequency is.

In the further course of the research it was found that the TTSP can indeed by extended by including the effect of the air void content. As a consequence, an air void-time-temperature superposition principle (AVTTSP) was introduced. Two shift factors take into account the test time and test frequency. By employing the AVTTSP the viscoelastic material reaction (dynamic modulus and phase lag) can be obtained for a wide range of air void contents at a user-defined reference temperature and reference frequency. Thus, the impact of a change in the air void content can be investigated for the tested material. The shape of the derived master curves is similar to those master curves derived from the TTSP. The shape resembles an S-shaped sigmoidal function. Thus, there are two threshold values in the low and high air void range, where the viscoelastic material parameters approximate an asymptotical value.

A comparison of both materials at a reference frequency of 10 Hz and a reference temperature of -10°C shows that clear differences can be found in terms of dynamic modulus only when the materials are tested in the 4PBB, whereas differences in terms of the phase lag become obvious in both test setups. The modified mix reacts stiffer in the intermediate air void range, more viscous in the intermediate and less viscous in the high air void range compared to the unmodified mix.

When the two test setups are compared it was found that they produce comparable dynamic moduli in the high air void range from 10.0% (v/v) on and comparable phase lags in the low air void range up to 10.0% (v/v). However, differences between both setups are not substantial outside of these ranges.

8 REFERENCES

Bell C.A., Hicks R.G., an Wilson J.E., “Effect of Percent Compaction on Asphalt Mixture Life”. ASTM STP829, American Society of Testing and Materials, Philadelphia, USA, 1984.

Di Benedetto H., Partl, M. N., Francken, L., and De La Roche, C., „Stiffness Testing for Bituminous Mixtures”. Journal of Materials and Structures, Vol. 34, 2001.

Findley W. N., Kasif O., and Lai J., “Creep and Relaxation of Nonlinear Viscoelastic Materials”, Dover Publications Inc., 1989.
Harrington E.T., “Significance of As-Constructed HMA Air Voids to Pavement Performance from Analysis of LTPP Data”. NCHRP Research Results Digest, Issue No. 269, Transport Research Board, Washington, USA, 2002.
Harvey J.S, Monismith C.L., and Eriksen K.T., “Effect of Laboratory Compaction Method on Test Results Using SHRP A-0003 Equipment”. Report Number: VTI 1A, Part 3, Swedish National Road and Transport Research Institute, VTI, Linköping, Sweden, 1994.
Kassem E., Masad E., Lytton R., and Chowdhury A., “Influence of Air Voids on Mechanical Properties of Asphalt Mixtures”. Journal of Road Materials and Pavement Design, Vol. 12, No.3, 2011.
Lytton R.L., Uzan J., Fernando E.G., Rogue R., Hiltmen D., and Stoffels S., “Development and Validation of Performance Prediction Models and Specifications for Asphalt Binders and Paving Mixtures”. SHRP A-357, Strategic Highway Research Program, Washington, USA, 1993.
Rowe G. M., Khoee S. H., Blankenship P., and Mahboub K. C., “Evaluation of Aspects of E* Test by Using Hot-Mix Asphalt Specimens with Varying Void Contents”. Journal of the Transport Research Boards No. 2127, Transport Research Board, Washington, USA, 2009.
Youngguk S., Omar E.-H., Mark K., Joon L, and Kim Y. R., “Air Void Models for Dynamic Modulus, Fatigue Cracking and Rutting of Asphalt Concrete”. Journal of Materials in Civil Engineering, Vol. 19, No. 10, 2007.